

ATMOS profile structure, filamentation, and transport around the 1994 Arctic proto-vortex

G. L. Manney,¹ H. A. Michelsen,² F. W. Irion,¹ M. R. Gunson,¹

Abstract

Many long-lived trace gas profiles observed by the Atmospheric Trace Molecule Spectroscopy (ATMOS) instrument around the developing polar vortex (the "proto-vortex") during early November 1994 show distinctive minimum/maximum pairs (laminae). High-resolution profiles calculated using a reverse trajectory (RT) model, initialized with tracers derived from ATMOS data mapped in potential vorticity/potential temperature coordinates, reproduce many of these laminae. High-resolution tracer maps from RT calculations show that inversions in ATMOS tracer profiles observed over eastern Asia arise from variations in the position of the vortex edge with altitude or from small horizontal scale variations in tongues of material drawn up from low latitudes around the proto-vortex edge. Laminae in ATMOS tracers around the proto-vortex tail (where the developing vortex extends out near 30°N latitude in a curved tail) arise from filamentation as material is drawn off the vortex edge. These narrow filaments drawn off the vortex edge may have very deep vertical extent, and where sampled at several levels by ATMOS, produce multiple laminae. Some laminae in the lower stratosphere are also evident in the ATMOS observations, arising from filamentation around the edge of the as-yet ill-defined proto-vortex region. The high-resolution maps from RT calculations initialized with ATMOS-based tracer fields show continuous filamentation around the proto-vortex throughout the stratosphere. The developing anticyclone was strongest and filamentation most vigorous in the middle stratosphere, where tongues of low-latitude and vortex air coiled up together in the anticyclone. The ability of the RT calculations to reproduce specific features, such as laminae, in the ATMOS trace gas observations confirms that these patterns seen in the RT maps are representative of the real atmosphere.

*stratospheric polar vortex
transport*

1. Introduction

Many modeling studies have shown the formation of small horizontal scale features around the polar vortex edge and in the anticyclone throughout the Arctic winter stratosphere [e.g., *Pierce and Fairlie*, 1993; *Waugh et al.*, 1994; *Sutton et al.*, 1994; *Manney et al.*, 1996, 1998; *Mariotti et al.*, 1997; *Harvey et al.*, 1999, and references therein]. *Orsolini* [1995] and *Schoeberl and Newman* [1995] showed that very deep filaments drawn off the winter polar vortex that tilt with height may lead to lamination in idealized tracer fields. Recent studies using observed trace-gas fields for model initialization have shown that laminae in trace gas profiles with a wide range of vertical scales can result both from filaments drawn off the vortex and from filaments drawn up around the polar vortex from low latitudes [e.g., *Orsolini et al.*, 1997, 1998; *Manney et al.*, 1998]. A theoretical study

by *Appenzeller and Holton* [1997] showed that tracer lamination resulting from differential advection by a vertically sheared wind field is expected at all levels along the edge of the winter polar vortex.

Most of the above studies focused on the Arctic winter and spring (December through March), after the polar vortex was fully developed. However, *Appenzeller and Holton* [1997] showed that tracer lamination is expected in the entire "winter half-year", and *Manney et al.* [1996] showed that filaments formed in calculated high-resolution idealized tracer fields in air drawn off the developing polar vortex (the "proto-vortex") and drawn up from low latitudes around the proto-vortex in early November 1994. It is typical in early winter to see material drawn off the vortex, and drawn in around the vortex from low latitudes [e.g., *Juckes and O'Neill*, 1988; *Manney et al.*, 1996, and references therein]. This process is thought to contribute to the formation of the main vortex/surf zone structure [e.g., *Juckes and O'Neill*, 1988] by strengthening potential vorticity (PV) and tracer gradients both along the vortex edge and in the subtropics. A

¹Jet Propulsion Laboratory/California Institute of Technology, Pasadena, California.

²Atmospheric and Environmental Research, Inc, San Ramon, California.

pattern reminiscent of the "Aleutian high", the anticyclonic feature over the date line that frequently persists for much of the NH winter [e.g., Harvey and Hitchman, 1996; Harvey et al., 1999, and references therein], often first begins to appear in late October or early November [Juckes and O'Neill, 1988; Harvey and Hitchman, 1996], although it remains transient until late December.

During the Atmospheric Laboratory for Applications and Science 3 (AT-3) mission in early November 1994, the Atmospheric Trace Molecule Spectroscopy (ATMOS) instrument observed middle and low latitudes in the northern hemisphere (NH) fall [Gunson et al., 1996], as the polar vortex was developing [e.g. Manney et al., 1996, 1999]. Many of these observations were around, both inside and outside, the proto-vortex edge [e.g. Michelsen et al., 1998; Manney et al., 1999]. Michelsen et al. [1998] showed that long-lived trace gas distributions observed inside the proto-vortex had distinct characteristics from those observed outside, and that some observations near, but outside, the proto-vortex were influenced by subtropical air. Individual ATMOS profiles observed in and around the proto-vortex in northern midlatitudes during AT-3 show complex vertical structure with large minima and/or maxima that appear to be correlated among a number of trace species measured simultaneously. Comparison with PV profiles for similar locations in many cases does not immediately reveal a dynamical explanation for many of these laminae in long-lived tracer profiles.

Manney et al. [1999] showed that the AT-3 ATMOS dataset provided good coverage of PV values typical of a wide range of dynamically distinct regions, from the tropics to inside the proto-vortex. This relatively complete coverage makes it possible to use ATMOS long-lived tracer fields as a function of PV to initialize high-resolution transport calculations. In the following, we use a reverse trajectory model to simulate high resolution tracer profiles and isentropic maps for the AT-3 ATMOS observations. These calculated fields are used to illustrate the transport of long-lived tracers around the developing polar vortex in fall, and to show that many previously unexplained laminae in the observed profiles arose from filaments with small horizontal scales that were sampled by ATMOS at certain altitudes. These filaments were continuously being drawn off the proto-vortex edge, and up around the proto-vortex from the subtropics during fall 1994.

2. Data and Analysis

The space shuttle-borne ATMOS instrument is a high-resolution Fourier transform infrared spectrometer that operates in solar occultation mode and simultaneously measures vertical profiles of approximately 30 species. ATMOS Ver-

sion 3 data cover altitudes ranging from ~ 6 to 80 km with a vertical resolution near 2 km. For each occultation during AT-3, the signal-to-noise ratio was optimized by the use of one of a set of four optical bandpass filters (numbered 3, 4, 9, and 12). N_2O and CH_4 , which we focus primarily on here, were measured in all filters, as was H_2O . The AT-3 data were taken during 3–12 November 1994, and the sunset observations covered ~ 4 – 50°N latitudes. Gunson et al. [1996] summarize the spatial coverage, filters used, and expected precision for each species. A discussion of the error budget for the Version 2 ATMOS data is given by Abrams et al. [1996]; as in Version 2, the precision of Version 3 ATMOS N_2O and CH_4 is typically near 5%, and that of H_2O near 10%. The Version 3 ATMOS data include separate estimates of the latitude and longitude of the observation at each altitude for which data are reported; these values may vary by as much as 5 – 10° between the bottom and top of some profiles, although most vary much less.

The United Kingdom Meteorological Office (UKMO) analyses [Swinbank and O'Neill, 1994], provided on a grid with ~ 2.5 – 3 km vertical resolution, were used to calculate PV, which was then interpolated to the locations of the ATMOS observations. A useful way to display sparse, irregularly spaced data such as those obtained by ATMOS is on isentropic (constant potential temperature, θ) surfaces (along which air moves in absence of diabatic effects) as a function of potential vorticity (PV) [e.g., Schoeberl et al., 1989, 1992] or equivalent latitude (the latitude that would enclose the same area as the corresponding PV contour) [e.g., Butchart and Remsberg, 1986; Lary et al., 1995; Manney et al., 1999, and references therein]. Such fields are frequently useful for model initialization [e.g., Lary et al., 1995; Manney et al., 1998, 1999]. Manney et al. [1999] described in detail the mapping of ATMOS trace gas observations into equivalent-latitude/ θ coordinates.

The model and methods used to simulate high-resolution maps and profiles at the ATMOS observation locations follow those described by Manney et al. [1998]. High-resolution trace-gas profiles and maps are obtained using a variation of the reverse-trajectory (RT) technique developed by Sutton et al. [1994]. UKMO horizontal winds and temperatures are used to drive the trajectory code described by Manney et al. [1994]. Since the three-dimensional (3D) version of the trajectory code is used here, all calculations include an estimate of diabatic descent. The trajectory code and its implementation using UKMO data are described in detail by Manney et al. [1994]. The RT technique [Sutton et al., 1994] involves trajectory calculations for parcels initially located at the positions and times at which the final calculated field is desired. A back-trajectory calculation is run for the ensemble of parcels to a time for which the initialization data are

available; the initialization data are then interpolated to the parcel positions. The mixing ratios of a tracer, assumed to be passively transported, at the locations where the trajectory calculations were initialized are given by this interpolated value. Thus the tracer field is effectively advected forward in time, although the trajectory calculation is done backwards. The resolution of the final field depends on the spacing of the parcel grid and the length of the back trajectory calculation [Sutton et al., 1994; Schoeberl and Newman, 1995].

We obtain high vertical resolution profiles by initializing parcels in a column centered over each ATMOS observation location, similar to the procedure used by Manney et al. [1998] and Manney et al. [1999]. The parcels are placed on 100 isentropic surfaces, equally spaced in $\log\theta$, between 380 and 2000 K (between ~ 13 -16 and 50-55 km); this corresponds to a vertical spacing (and therefore a best vertical resolution) of ~ 350 -400 m, about 5-6 times better than the ATMOS observations. The ATMOS observation latitudes and longitudes for each profile are interpolated to the model θ levels to determine the central location of the array of parcels at each level. An 11 by 11 array of parcels centered around this location is placed in a 2° longitude by 1° latitude (~ 50 km per side at midlatitudes) box at each level. The profiles shown below are constructed from the average of the 121 parcels at each level; comparisons with profiles reconstructed from individual parcels were used to verify that we did not see any large changes in behavior over the small area of the column of initialized parcels [Manney et al., 1998]. High-resolution maps were made on selected isentropic surfaces (with θ values selected from the set of 100 levels on which the profiles were generated) using the same RT procedure, but initializing the parcels on an equal area grid with 0.8° latitude spacing, and 0.8° longitude spacing at the equator (~ 80 by 80 km). The resulting high resolution fields are interpolated to a 0.8° latitude by 1.8° longitude grid for plotting. All of the RT calculations shown here are for 7-8 days, with the trajectory calculations initialized at the nearest half-hour (the trajectory time-step) to the ATMOS observation time for that profile.

The primary trace gas fields used as initialization data are obtained from the ATMOS AT-3 data mapped into equivalent-latitude/ θ space, as described by Manney et al. [1999]; UKMO PV for the initialization day (the ending or earliest day of the back-trajectory calculations) is used to reconstruct a spatial field. As shown by Manney et al. [1999], meteorological conditions in the NH during AT-3 were such that the ATMOS observations covered approximately 0 - 60° equivalent latitude. This coverage allows us to produce RT tracer maps that fully cover the region outside and just inside the proto-vortex, where filamentation is occurring. This range is also such that essentially all of the air at the locations

sampled by ATMOS was advected from regions (in equivalent latitude) also sampled by ATMOS, thus giving complete simulated high resolution profiles for all of the cases studies. Since the initialization tracer data are derived from the ATMOS data themselves, general agreement between the overall very large scale structure of the calculated and observed profiles is expected. However, since the ATMOS equivalent-latitude/ θ fields involve averaging many observations (in the region of interest here, there are typically ~ 15 to over 40 ATMOS-observed points in each PV/ θ bin used for the gridding [Manney et al., 1999]), they are greatly smoothed. Profiles reconstructed using the low-resolution UKMO PV with the ATMOS equivalent-latitude/ θ fields thus typically show only those features with both horizontal and vertical dimensions, and time persistence, large enough to be captured in the UKMO PV fields. By using these fields to initialize high-resolution transport calculations, we can estimate what smaller-scale structures may be produced via advection by the large-scale wind fields.

To check on the robustness of specific features in the simulated profiles, we have also constructed RT profiles of N_2O , CH_4 , and H_2O using the Upper Atmosphere Research Satellite (UARS) based "climatologies" described by Manney et al. [1999] for initialization. These are global equivalent-latitude/ θ fields constructed for 10 times spaced throughout a year from Cryogenic Limb Array Etalon Spectrometer (CLAES) N_2O and CH_4 [Roche et al., 1996] and Microwave Limb Sounder (MLS) H_2O [Pumphrey, 1998] data from late April 1992 through early April 1993 averaged over six days, and assigned to the central day of the averaging period. An initialization field for a particular day is constructed using UKMO PV for that day and the appropriate linear interpolation in time between neighboring UARS-based equivalent-latitude/ θ fields. While there are known biases between CLAES or MLS and ATMOS data [Roche et al., 1996; Pumphrey, 1998], and further biases may be expected due to interannual variability and the averaged nature of the UARS-based equivalent-latitude/ θ fields, comparing profiles obtained from reconstruction with the low resolution UKMO PV and from the RT calculations with those obtained in corresponding manners using the ATMOS equivalent-latitude/ θ fields provides a check on the general appearance of structure generated in the calculations. The CLAES N_2O and CH_4 used to construct these climatologies are reliable only down to ~ 550 K for the season and latitudes we are focusing on [e.g., Roche et al., 1996].

3. Results

Plate 1 shows ATMOS N_2O and CH_4 profiles for occultation SS07, taken on 4 Nov 1994. Two notable features

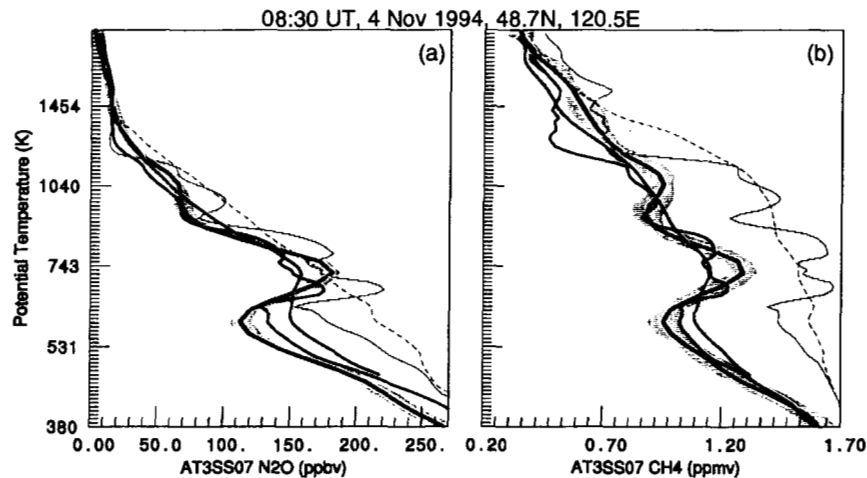


Plate 1. (a) N_2O (ppbv) and (b) CH_4 (ppmv) mixing ratios for ATMOS profile SS07, on 4 Nov 1994. The thick black line shows the ATMOS observed values, with the surrounding grey shading indicating the associated uncertainty. The green line shows the profile reconstructed from the (low resolution) UKMO PV and the ATMOS equivalent-latitude/ θ tracer field. The blue line shows the results of the RT calculation initialized with the reconstructed ATMOS data. The dashed and solid grey lines show the low resolution reconstruction and RT calculation results using the UARS-based climatology for tracer initialization. See text for details.

in the ATMOS profiles are a deep minimum and maximum near 600 and 700 K, respectively, and another minimum and maximum near 900 and 1050 K, respectively. As is the case for all the features presented in this study, these features are correlated in N_2O and CH_4 . Although individual ATMOS H_2O profiles frequently contain spurious wave-like structure [e.g., Abbas *et al.*, 1996], minima and maxima in SS07 H_2O that are anti-correlated (since H_2O increases toward the pole) with those in N_2O and CH_4 (since H_2O increases toward the pole) are also apparent (not shown). In the profiles reconstructed from ATMOS equivalent-latitude/ θ fields and UKMO PV (green lines), there is a shoulder in the profile near the level of the lower maximum, indicating that some of the structure resulting in this feature is of large enough scale to appear in the averaged ATMOS fields and/or the UKMO PV fields. There is, however, no indication of a feature resembling the upper minimum/maximum pair.

The calculated high-resolution profiles from both ATMOS and CLAES based initializations show a distinct minimum near 900 K, similar to that seen in the ATMOS observations, although the maximum above it in the high-resolution ATMOS based profiles is not as large. The minimum and maximum near 600 and 700 K in the RT profiles also appear more similar to those in the observations, although there is a secondary minimum in the calculated profiles that does not show up in the ATMOS data, possibly due to limitations in the ATMOS vertical resolution.

Plate 2 shows the origins of the laminae in the RT profiles. At all levels shown, the ATMOS SS07 observations were in the proto-vortex edge region at a longitude near where a tongue of low-latitude air was beginning to curve up around the vortex, where tracer gradients were strong. At 989 K, the observations were in a tongue of high CH_4 drawn up from low latitudes (Plate 2a), whereas at 909 K (Plate 2b) the ATMOS observations were toward the inside of the vortex edge region, where CH_4 was lower. As noted by Fairlie *et al.* [1997], high-resolution transport calculations such as these are useful for refining large-scale gradients along the vortex edge, and thus give a clearer indication of the position of the strong gradient region. The RT calculations in this case indicate that the ATMOS observations near 900 K were farther into the vortex than suggested by the UKMO PV, and thus at lower CH_4 values. The smaller maximum in the ATMOS-RT profiles than in the observations near 1000 K may result from inaccuracies in the position of the filament of high CH_4 in the RT calculations – if the maximum tracer in the filament were slightly poleward, much higher tracer values would have been obtained. An RT map constructed using the CLAES-based initialization fields shows the highest tracer region in the tongue extending farther toward the poleward side of the tongue, resulting in the larger maximum (with respect to the low resolution reconstruction from the same fields) near 1000 K in the CLAES-RT profile (Plate 1b).

Plates 2c and d show the origins of the lower mini-

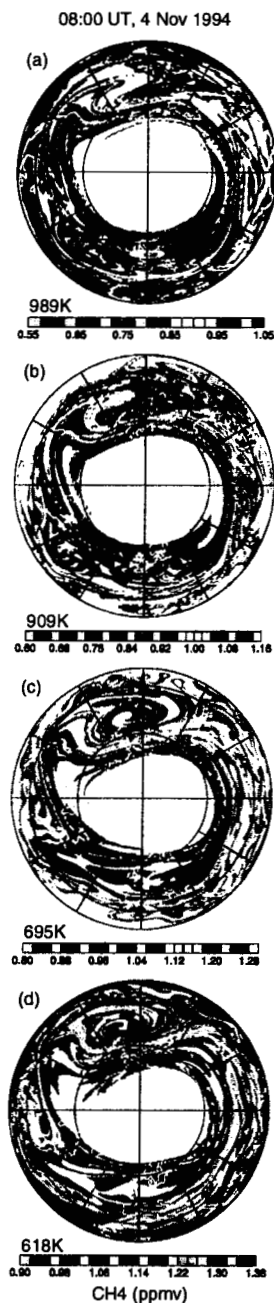


Plate 2. High resolution NH maps of CH_4 from RT calculations initialized with ATMOS equivalent-latitude/ θ fields (see text) for 08:30 UT, 4 Nov 1994, near the observation time of SS07. Levels shown are (a) 989 K, (b) 909 K, (c) 695 K, and (d) 618 K. The black triangle indicates the position of SS07. The map projection is orthographic, with 0° longitude at the bottom and 90°E to the right. The domain is from equator to pole, with thin dashed lines at 30° and 60°N . Note that the contour interval is different at different levels, to emphasize the horizontal structure in the fields.

imum/maximum pair in SS07. At 695 K the SS07 observations were in a large tongue of material drawn up around the vortex edge, while at 618 K they were towards the interior of the vortex edge region. While the wide tongue drawn around the vortex seen in Plate 2c is broad enough to be apparent in the low resolution PV fields, and thus a shallow maximum appears in the profiles reconstructed from those fields, the RT calculations show the interior of this large tongue to be non-homogeneous, including several small narrow filaments of even higher CH_4 . These small filaments result in the higher maximum seen in Plate 1b. The RT calculations also produce a value of the minimum closer to that observed in SS07, indicating that the RT calculations more fully capture the sharpness of the PV and tracer gradients along the vortex edge.

Plate 3 shows CH_4 and H_2O from ATMOS profile SS40, along with the corresponding calculated profiles. SS40 CH_4 shows a minimum/maximum pair at $\sim 600/710$ K and another in the upper stratosphere at $\sim 1100/1430$ K. Corresponding maximum/minimum features are seen in ATMOS H_2O . For both CH_4 and H_2O (and N_2O , not shown), there is little indication of either feature in the profiles reconstructed from low resolution PV data, except for a slight minimum in CH_4 near 1100 K. The ATMOS-RT calculations, however, show very good agreement with the lower minimum/maximum pair in CH_4 and fairly good agreement with the corresponding maximum/minimum pair in H_2O ; the CLAES (CH_4) and MLS (H_2O) based RT calculations also show corresponding variations. In addition, the profiles from the RT calculations show a distinct maximum near 1430 K, similar to that seen in the ATMOS profiles.

Plate 4 shows how the laminae in the SS40 RT CH_4 profiles arise. In both the middle and the upper stratosphere, the SS40 observations were in the vicinity of a relatively narrow tail of material being pulled off the vortex edge. Near 1100 K (Plate 4b), the ATMOS observations were in a relatively wide portion of the tail, with very low tracer values representative of air from well inside the proto-vortex. At 1430 K (Plate 4a), the tail drawn off the vortex has been sheared out, and parts of it folded back upon itself with higher CH_4 air from the edge region; the SS40 observations were located along one of these filaments of higher CH_4 . Whereas the minimum was apparent in the low resolution reconstructed profiles because the tail of the proto-vortex was relatively wide at that level, the maximum results from a filament that was not present in the low resolution tracer fields. The appearance of such a feature in the ATMOS tracer fields strongly suggests that a similar filament was present in the real atmosphere.

The tail drawn off the vortex is narrower at lower levels (Plate 4c, d), as has been seen in previous studies of the

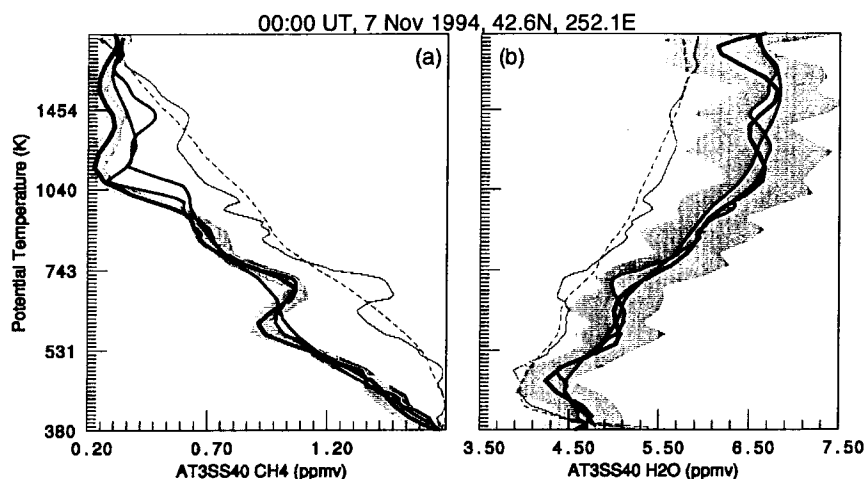


Plate 3. (a) CH₄ (ppmv) and (b) H₂O (ppmv) mixing ratios for ATMOS profile SS40, on 6 Nov 1994. Layout and line styles are as in Plate 1.

vertical structure of vortex filaments [Schoeberl and Newman, 1995]. In addition to the tail being pulled off, large tongues of low latitude, high CH₄ air were drawn in around the vortex, and coiled up with air from the tail in the developing anticyclone. Near 700 K, SS40 was located in the cusp where the tail drawn off the vortex first curved around the high-CH₄ material drawn in from low latitudes, in a region of high CH₄. Near 600 K, the ATMOS observation was in the filament of low CH₄ pulled off the vortex. In the UKMO PV fields, since neither this tongue, nor the cusp region are well-defined in the UKMO PV fields, the low resolution reconstructed profiles show the CH₄ at both levels to have moderate values characteristic of air from the outside of the vortex edge region.

As well as the features discussed above, the ATMOS H₂O profile in Plate 3b shows an additional minimum in H₂O in the lower stratosphere near 480 K. At this level the vertical gradient in CH₄ is very stronger, and thus smaller variations such as this feature would produce in CH₄ may not be immediately apparent. Although this minimum was apparent in the low resolution reconstructed profiles, it is deeper and more closely resembles the ATMOS observations in the RT profiles. Plate 5 shows the origin of this feature. At this time in the NH fall, the lower stratospheric vortex is just beginning to develop [e.g., Manney et al., 1999], and large scale tracer gradients are relatively weak. There is, however, a good deal of stirring and filamentation in mid-latitudes. The SS40 observations were made in a region where a broad filament of low latitude, low H₂O air had been drawn in and was coiled up with air high in H₂O from the incipient vortex. This feature in the H₂O profile was thus en-

hanced by the seasonal cycle in tropical water vapor, which demonstrated a minimum near this level in tropical profiles [e.g., Abbas et al., 1996]. Although the low-H₂O tongue was broad enough to be apparent in fields reconstructed using low-resolution PV, the RT calculations indicate that the minimum values in this tongue were in fact lower than indicated in the low-resolution fields. Even though the flow at this level is considerably less organized than at higher levels, the overall pattern seen here can be recognized as the extension of the one seen at higher levels where air is drawn off the proto-vortex and coiled up in the developing anticyclone with air drawn in from low latitudes.

Plate 6 shows CH₄ profiles for SS64. The ATMOS profile shows two pairs of minima and maxima in the lower stratosphere, near 480/515 K and 670/730 K, and a deep minimum in the upper stratosphere near 1170 K. The low resolution reconstructed profiles show none of these features. The ATMOS-RT profiles have a deep minimum in the upper stratosphere, and a minimum and maximum strongly resembling those near 670 and 730 K; there is also a maximum and minimum near the lowest pair, although the minimum is not as deep and the maximum is at a slightly lower level than in the ATMOS profile.

Plate 7a shows that the deep minimum in the upper stratosphere results from a very narrow filament of proto-vortex air drawn off its edge. This is the upward extension of a still narrow, but slightly wider filament seen at 731 K (Plate 7b) and 672 K (Plate 7c). At 731 K, the ATMOS observations were in a filament of low latitude air drawn poleward of this vortex filament; at 672 K, the ATMOS observations were in the vortex filament. This is another example of a

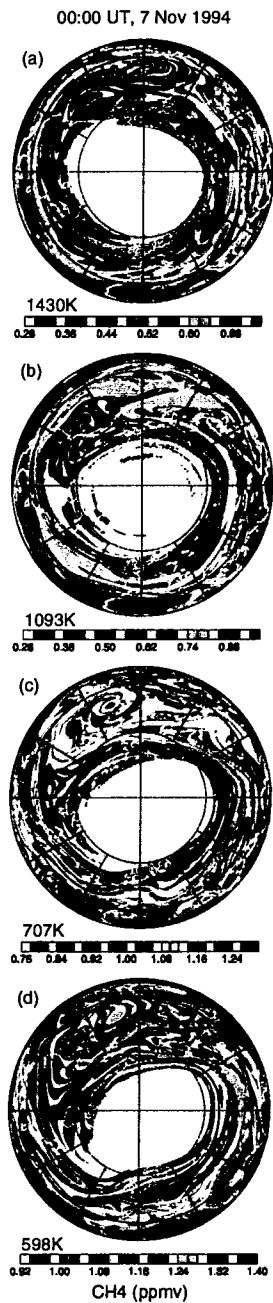


Plate 4. As in Plate 2, but for SS40, 00:00 UT, 7 Nov 1994. Levels shown are (a) 1430 K, (b) 1093 K, (c) 707 K, and (d) 598 K. Layout is as in Plate 2.



Plate 5. As in Plate 4, but for RT H₂O at 481 K. Layout is as in Plate 4.

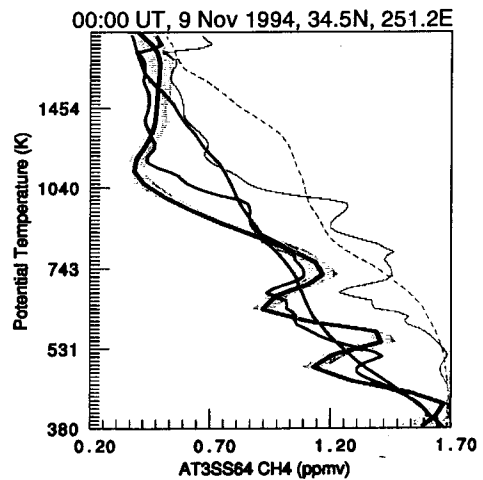


Plate 6. CH₄ (ppmv) mixing ratios for ATMOS profile SS64, on 9 Nov 1994. Layout and line styles are as in Plate 1.

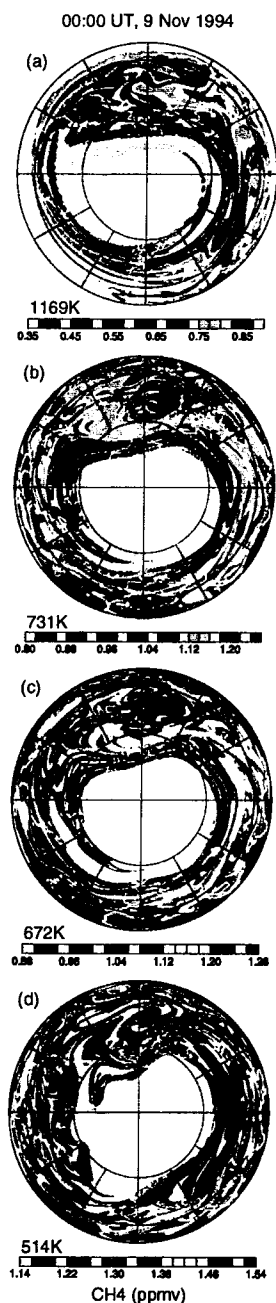


Plate 7. As in Plate 2, but for SS64, 00:00 UT, 9 Nov 1994. Levels shown are (a) 1169 K, (b) 731 K, (c) 672 K, and (d) 514 K. Layout is as in Plate 2.

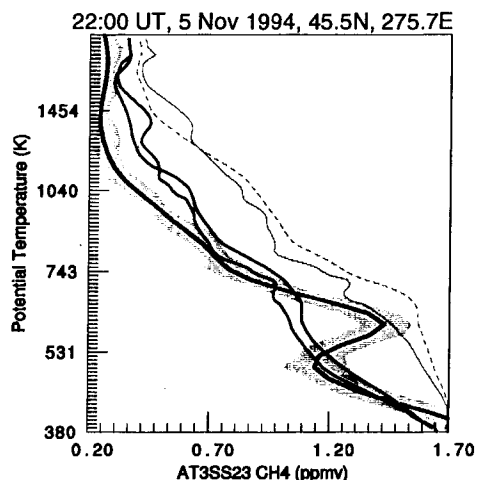


Plate 8. CH₄ (ppmv) mixing ratios for ATMOS profile SS23, on 5 Nov 1994. Layout and line styles are as in Plate 1.

horizontally-narrow but very deep filament. This filament is no longer apparent at 514 K; the maximum in the RT profile there arises from a tongue of low latitude, high-CH₄ air drawn up around the vortex edge, producing extremely strong tracer gradients. At 480 K (not shown), the observations were on the poleward side of this high-CH₄ tongue, giving rise to the minimum in the RT profile. *Manney et al.* [1998] showed several examples where laminae in ozone profiles were reproduced by RT calculations with an offset in altitudes; these were particularly common in cases with extremely strong tracer gradients, such as seen here, where a slight error in the position of a feature such as the tongue of high-CH₄ air could lead to a large difference in tracer values.

The above cases are representative examples of structures in ATMOS long-lived tracer profiles that can be explained by examination of the small horizontal scale features that are produced by the large-scale wind fields. Similar features are seen in many other ATMOS profiles observed in the NH in November 1994, especially in those taken in the entrance region where low latitude air was first drawn up around the proto-vortex (e.g., SS07, Plates 1 and 2) or in the proto-vortex tail region (e.g., SS40, SS64, Plates 3 through 7). There are also, however, a few cases where the RT calculations fail to reproduce laminar structure seen in ATMOS profiles. Plate 8 shows one such case, for profile SS23. Although there is a deep minimum/maximum pair in the ATMOS profile near 500/600 K, none of the reconstructed or RT profiles show evidence of a significant feature here. The feature in the ATMOS data is robust, with a similar feature appearing in N₂O and an anti-correlated feature in H₂O;

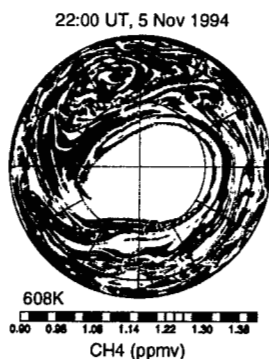


Plate 9. As in Plate 2, but for SS23, 22:00 UT, 5 Nov 1994, at 608 K.

RT calculations initialized with those species also fail to reproduce the lamina. A similar feature was seen in ATMOS observations taken near the same location approximately 2 days later, and that feature was apparent in RT calculations. Plate 9 shows an RT CH_4 map at 608 K for the time of this observation, with the location of SS23 indicated. A large tongue of low-latitude air was drawn up around the vortex edge, which extended in a tail out to near 30°N , similar to the situation seen at lower levels for SS64 (Plate 7). This tongue is quite deep, extending from below 500 K to about 750 K, and the RT calculations show SS23 to be poleward of it at all levels. Given the consistency between species, and the occurrence of similar features near the SS23 location at different times, it is unlikely that the lamina in SS23 is a spurious feature in the ATMOS data; however, it is certainly plausible that, if the RT calculations give a slightly erroneous position for the tongue of low latitude air, ATMOS may have sampled air from this tropical tongue near 600 K. Comparison of N_2O and CH_4 correlations near the altitude of the lamina for SS23 with the tropical and midlatitude curves derived by Michelsen et al. [1998] shows that, while the SS23 data in general fall on the midlatitude curve, the data at levels near 600 K fall on the tropical curve, further evidence that ATMOS sampled material from this tongue. Although initializations using both ATMOS and UARS-based equivalent-latitude/ θ fields, and several trace gases all failed to reproduce this feature, all of these initializations depend on the same low-resolution PV field; thus, a mis-representation of the position of the tongue of low latitude air could result either directly from inaccuracies in the winds used for the RT calculations, or from advection of a feature that was inaccurately represented in the initialization field reconstructed using UKMO PV.

The ability of the RT calculations to reproduce many of the features seen in individual ATMOS profiles indicates that many of the specific small horizontal scale features seen in

the RT maps shown in Plates 2, 4, 5, 7, and 9 correspond to features that were present in the atmosphere in early November 1994. Having verified that these calculated maps show realistic structure, the maps shown above for levels throughout the stratosphere illustrate the three-dimensional structure of the proto-vortex and transport of tracers around it in early November 1994. A feature resembling the Aleutian high was present throughout the AT-3 mission [Manney et al., 1999]; associated with this feature are tongues of low latitude air drawn up around the vortex (curving around the proto-vortex near 150°E) and tails of vortex air drawn off near 240°E that subsequently coil up together in the anticyclone. The anticyclonic feature is strongest in the middle stratosphere, between ~ 600 and 800 K (Plates 2c and d, 4c and d, 7b and c, and 9). At higher levels, the proto-vortex was more symmetric, the anticyclonic feature less pronounced, and continuous coiling up together of low latitude and vortex air was not apparent (Plates 2a and b, 4a and b, and 7a). Stratospheric minor warmings in early winter have been noted to frequently be strongest in the middle stratosphere, typically producing the largest shift of the vortex off the pole and hence the strongest anticyclone there [e.g., Labitzke, 1977; Juckes and O'Neill, 1988]; the pattern of the flow during AT-3 was like that during such events.

In the lower stratosphere (Plates 5 and 7d), the polar vortex was only beginning to form and PV gradients were still relatively weak [Manney et al., 1999]. Although the lower stratospheric vortex is not yet well-defined, it is apparent from Plates 5 and 7d that the pattern of coiling up of low latitude and vortex air in the anticyclone region extends into the lower stratosphere. In addition to the features mentioned above, in the middle and lower stratosphere (below ~ 700 K), a tongue of low latitude air was drawn up around the tail of the vortex, near 270°E (Plates 2c and d, 4c and d, 7c and d, and 5), frequently poleward of additional filaments of air drawn off the vortex edge (e.g., near 300° to 330°E in Plates 4c and d). The overall picture of the developing polar vortex in early November 1994 shows an already well-defined vortex in the middle and upper stratosphere, surrounded by a very dynamic region with air continuously being pulled off the proto-vortex and drawn up from low latitudes, resulting in a large degree of filamentation and mixing of air with disparate tracer values in midlatitudes. These patterns of filamentation and mixing extended into the lower stratosphere, even though the vortex was not yet well-defined there.

4. Discussion and Conclusions

Reverse trajectory (RT) calculations, initialized with tracers reconstructed from equivalent-latitude/ θ fields based on

ATMOS observations [Manney et al., 1999], have been used to explore the origins of large laminae in ATMOS profiles observed during the AT-3 mission in the northern hemisphere fall in early November 1994, and to illustrate the structure and evolution of the proto-vortex and long-lived tracers at this time. Many of the profiles observed in NH midlatitudes ($\sim 30^\circ$ – 50° N) during AT-3 show distinctive large laminae, which are apparent in all long-lived gases observed by ATMOS. These most commonly appear in the middle stratosphere, near 600–800 K, but there are also a number of instances of laminae in both the upper and the lower stratosphere.

During AT-3, the polar vortex was in the process of developing, with a distinct “proto-vortex” present in the middle and upper stratosphere (above ~ 600 K), and an anticyclone developing in the “Aleutian high” region [Manney et al., 1999]. Laminae were most commonly seen in ATMOS profiles taken in two areas: 1) between $\sim 90^\circ$ and 150° E, in the entrance region where low latitude material is first being drawn up around the vortex edge, and 2) between $\sim 220^\circ$ and 300° E, where the vortex extended out to near 30° N, and a tail of material was being drawn off its edge and subsequently coiling up in the developing anticyclone with the low latitude air drawn in from region 1. Additional filaments of low latitude air were drawn up around the vortex edge in region 2, along the equatorward side of the proto-vortex tail.

Comparison of high vertical resolution tracer (CH_4 , N_2O , and H_2O) profiles and high horizontal resolution maps constructed using the RT calculations shows that laminae in ATMOS tracers profiles in region 1, the main entrance region for low-latitude air flowing up around the proto-vortex edge, arise from both structure in the vortex edge, such that the position of the region of very strong tracer gradients varies with altitude, and from small horizontal scale variations in the tongue of material drawn up from low latitudes. While some features arising from crossing the vortex edge are apparent in a blurred form in profiles reconstructed from low resolution PV fields, the RT calculations refine the representation of tracer gradients along the vortex edge, and improve the agreement between observed and calculated profiles. Features arising from small scale structure in the low latitude tongue are typically not represented in low resolution reconstructions or PV fields.

Laminae in ATMOS tracers in the proto-vortex tail region (region 2 above) typically arise from filamentation occurring as air is drawn off the vortex edge, either from the end of the tail, or in narrow filaments along the side of the tail. We have shown examples where narrow filaments drawn off the vortex edge in this region have very deep vertical extent, from ~ 600 to 1200 K, and were sampled at several levels by ATMOS, producing multiple laminae in some profiles.

The development of vortex filaments with very deep vertical structure was noted during NH winter by Schoeberl and Newman [1995] in a study of fine-scale transport of idealized tracers. Our calculations show that deep, narrow vortex filaments are also common in fall, and the ATMOS observations provide observational evidence for their presence in early November 1994. Laminae also arise in the proto-vortex tail region in the lower stratosphere, due to filamentation around the edge of the as-yet only roughly defined proto-vortex region; such filaments are not as deep as those seen in the middle and upper stratosphere where the vortex is better defined, but evidence in the ATMOS profiles indicates that such features are captured in the observations.

Some cases were seen where the RT calculations failed to reproduce laminae that were robust features in the ATMOS observations. It was generally found in such cases that there were features in the RT maps that could have produced such laminae, but these features were slightly offset from the position of the ATMOS observations. This observation suggests that such failures may be due to inaccuracies in the RT transport calculations, either in the winds themselves, or in the PV used to reconstruct the initialization fields.

High-resolution maps from RT calculations initialized using the equivalent-latitude/ θ mapped ATMOS data give us a picture of the developing vortex in early November 1994 that shows low-latitude material being continuously drawn up around the proto-vortex and mixing in the region of the developing anticyclone, with vortex air drawn in narrow filaments off the tail. This process was most vigorous and continuous in the middle stratosphere where the anticyclone was strongest, but also extended into the lower stratosphere where the vortex was not yet well-defined. Throughout the stratosphere the proto-vortex was surrounded by a region where continuous filamentation was occurring. The agreement between the structure seen in the RT calculations and many features observed by ATMOS confirms this picture of a very dynamic, variable, and highly structured proto-vortex in the NH fall.

Acknowledgments. We thank the ATMOS and CLAES instrument teams for their role in producing the datasets used here, especially H. C. Pumphrey for production of the MLS H_2O retrievals and J. B. Kumer, J. L. Mergenthaler and A. E. Roche for CLAES data, and the UKMO (R. Swinbank and A. O’Neill) for meteorological data. Work at the Jet Propulsion Laboratory, California Institute of Technology was done under contract with the National Aeronautics and Space Administration. HAM was supported by the NASA Atmospheric Chemistry, Modeling, and Analysis Program (NAS1-98118).

References

- Abbas, M. M., et al., Seasonal variations of water vapor in the lower stratosphere inferred from ATMOS/ATLAS-3 measurements of H₂O and CH₄, *Geophys. Res. Lett.*, *23*, 2401–2404, 1996.
- Abrams, M. C., et al., On the assessment and uncertainty of atmospheric trace gas burden measurements with high resolution infrared solar occultation spectra from space by the ATMOS experiment, *Geophys. Res. Lett.*, *23*, 2337–2340, 1996.
- Appenzeller, C., and J. R. Holton, Tracer lamination in the stratosphere: a global climatology, *J. Geophys. Res.*, *102*, 13,555–13,569, 1997.
- Butchart, N., and E. E. Remsburg, The area of the stratospheric polar vortex as a diagnostic for tracer transport on an isentropic surface, *J. Atmos. Sci.*, *43*, 1319–1339, 1986.
- Fairlie, T. D. A., R. B. Pierce, W. L. Grose, G. Lingenfelter, M. Loewenstein, and J. R. Podolske, Lagrangian forecasting during ASHOE/MAESA: Analysis of predictive skill for analyzed and reverse-domain-filled potential vorticity, *J. Geophys. Res.*, *102*, 13,169–13,182, 1997.
- Gunson, M. R., et al., The Atmospheric Trace Molecule Spectroscopy (ATMOS) experiment: Deployment on the ATLAS Space Shuttle missions, *Geophys. Res. Lett.*, *23*, 2333–2336, 1996.
- Harvey, V. L., and M. H. Hitchman, A climatology of the Aleutian high, *J. Atmos. Sci.*, *53*, 2088–2101, 1996.
- Harvey, V. L., M. H. Hitchman, R. B. Pierce, and T. D. Fairlie, Tropical aerosol in the Aleutian high, *J. Geophys. Res.*, *104*, 6281–6290, 1999.
- Juckes, M. N., and A. O'Neill, Early winter in the northern hemisphere, *Q. J. Roy. Meteor. Soc.*, *114*, 1111–1125, 1988.
- Labitzke, K., Interannual variability of the winter stratosphere in the northern hemisphere, *Mon. Wea. Rev.*, *105*, 762–770, 1977.
- Lary, D. J., M. P. Chipperfield, J. A. Pyle, W. A. Norton, and L. P. Riishojgaard, Three-dimensional tracer initialization and general diagnostics using equivalent PV latitude-potential-temperature coordinates, *Q. J. Roy. Meteor. Soc.*, *121*, 187–210, 1995.
- Manney, G. L., R. W. Zurek, A. O'Neill, and R. Swinbank, On the motion of air through the stratospheric polar vortex, *J. Atmos. Sci.*, *51*, 2973–2994, 1994.
- Manney, G. L., R. Swinbank, and A. O'Neill, Stratospheric meteorological conditions for the 3–12 Nov 1994 ATMOS/ATLAS-3 measurements, *Geophys. Res. Lett.*, *23*, 2409–2412, 1996.
- Manney, G. L., J. C. Bird, D. P. Donovan, T. J. Duck, J. A. White-way, S. R. Pal, and A. I. Carswell, Modeling ozone laminae in ground-based Arctic wintertime observations using trajectory calculations and satellite data, *J. Geophys. Res.*, *103*, 5797–5814, 1998.
- Manney, G. L., H. A. Michelsen, M. L. Santee, M. R. Gunson, F. W. Irion, A. E. Roche, and N. J. Livesey, Polar vortex dynamics during spring and fall diagnosed using ATMOS trace gas observations, *J. Geophys. Res.*, *accepted*, 1999.
- Mariotti, A., M. Moustaooui, B. Legras, and H. Teitelbaum, Comparison between vertical ozone soundings and reconstructed potential vorticity maps by contour advection with surgery, *J. Geophys. Res.*, *102*, 6131–6142, 1997.
- Michelsen, H. A., G. L. Manney, M. R. Gunson, C. P. Rinsland, and R. Zander, Correlations of stratospheric abundances of CH₄ and N₂O derived from ATMOS measurements, *Geophys. Res. Lett.*, *25*, 2777–2780, 1998.
- Orsolini, Y. J., On the formation of ozone laminae at the edge of the arctic polar vortex, *Q. J. Roy. Meteor. Soc.*, *121*, 1923–1941, 1995.
- Orsolini, Y. J., G. Hansen, U. Hoppe, G. Manney, and K. Fricke, Dynamical modelling of wintertime lidar observations in the arctic: ozone laminae, and ozone depletion, *Q. J. Roy. Meteor. Soc.*, *123*, 785–800, 1997.
- Orsolini, Y. J., G. L. Manney, A. Engel, J. Ovarlev, C. Claud, and L. Coy, Layering in halocarbons, methane, nitrous oxide and water vapour over mid-latitudes, *J. Geophys. Res.*, *103*, 5815–5825, 1998.
- Pierce, R. B., and T. D. A. Fairlie, Chaotic advection in the stratosphere: implications for the dispersal of chemically-perturbed air from the polar vortex, *J. Geophys. Res.*, *98*, 18,589–18,595, 1993.
- Pumphrey, H. C., Nonlinear retrievals of water vapour from the UARS Microwave Limb Sounder (MLS), *Adv. Sp. Res.*, *21*, 389–392, 1998.
- Roche, A. E., et al., Validation of CH₄ and N₂O measurements by the Cryogenic Limb Array Etalon Spectrometer instrument on the Upper Atmosphere Research Satellite, *J. Geophys. Res.*, *101*, 9679–9710, 1996.
- Schoeberl, M. R., and P. A. Newman, A multiple-level trajectory analysis of vortex filaments, *J. Geophys. Res.*, *100*, 25,801–25,815, 1995.
- Schoeberl, M. R., et al., Reconstruction of the constituent distribution and trends in the Antarctic polar vortex from ER-2 flight observations, *J. Geophys. Res.*, *94*, 16,815–16,845, 1989.
- Schoeberl, M. R., L. R. Lait, P. A. Newman, and J. E. Rosenfield, The structure of the polar vortex, *J. Geophys. Res.*, *97*, 7859–7882, 1992.
- Sutton, R. T., H. MacLean, R. Swinbank, A. O'Neill, and F. W. Taylor, High-resolution stratospheric tracer fields estimated from satellite observations using Lagrangian trajectory calculations, *J. Atmos. Sci.*, *51*, 2995–3005, 1994.
- Swinbank, R., and A. O'Neill, A stratosphere-troposphere data assimilation system, *Mon. Wea. Rev.*, *122*, 686–702, 1994.
- Waugh, D. W., et al., Transport out of the lower stratospheric Arctic vortex by Rossby wave breaking, *J. Geophys. Res.*, *99*, 1071–1088, 1994.

G. L. Manney (e-mail: manney@mls.jpl.nasa.gov, Mail Stop 183-701), M. R. Gunson (Mail Stop 169-237), F. W. Irion (Mail Stop 183-601), Jet Propulsion Laboratory, Pasadena, CA 91109.

H. A. Michelsen, Atmospheric and Environmental Research, Inc., 2682 Bishop Dr., Ste 120, San Ramon, CA 94583